Available online at www.sciencedirect.com
ScienceDirect
Journal of Power Sources 162 (2006) 239–245
JOURNAL OF POWER SOURCES
www.elsevier.com/locate/jpowsour

Experimental characterization and modeling of commercial polybenzimidazole-based MEA performance

Anders R. Korsgaard [a,*], Rasmus Refshauge [b], Mads P. Nielsen [a], Mads Bang [a], Søren K. Kær [a]

[a] *Institute of Energy Technology, Aalborg University, DK-9220 Aalborg, Denmark*
[b] *DK-8600 Silkeborg, Denmark*

Received 30 January 2006; received in revised form 15 June 2006; accepted 16 June 2006
Available online 30 August 2006

Abstract

High temperature polymer fuel cells based on polybenzimidazole membranes (PBI) operated at 100–200 °C are currently receiving much attention in relation to fuel cell reforming systems due to two main reasons. At first they have proven to have excellent resistance to high CO concentrations, which decreases the number of system components in the fuel processing system. The preferential oxidation reactors can be left out and in addition a water condenser is not required. These system simplifications additionally decrease the parasitic losses associated with the components.

However, insufficient data are currently published to enable good system design and modeling. In this paper the influence of operation on synthesis gas and the variation of the cathode stoichiometry are investigated based on a generic commercial membrane electrode assembly (MEA). The CO content in the anode gas was varied from 0 to 5%, with CO_2 contents ranging from 25 to 20% at temperatures ranging from 160 to 200 °C. The influence of the cathode stoichiometry was investigated in the interval of 2–5 at temperatures from 120 to 180 °C with pure hydrogen on the anode.

A novel semi empirical model of the fuel cell voltage versus current density, cathode stoichiometry and temperature was derived. It shows excellent agreement with the experimental data. The simplicity and accuracy of the model makes it ideal for system modeling, control design and real-time applications.

Keywords: Fuel cell; PEM; PBI; Intermediate temperature; Modeling; HTPEM

1. Introduction

High temperature polymer fuel cells are receiving increasing attention for several reasons. First of all, the high operating temperature allows a simple fuel processing system. This is due to the fact that CO-desorption is favored at higher temperatures resulting in decreased CO-coverage of the electrochemically active Pt sites. Moreover, better heat integration with the reforming system is possible as no water condensing system is necessary between the reformer and the fuel cell. The membrane electrode assembly (MEA) does not need any external humidification allowing simpler system design leaving out expensive and bulky humidifiers. Additionally, the pressure loss in the fuel cell stack itself can be reduced because no liquid water has to be forced out of the cell. This in turn decreases the parasitic energy need for driving the air blower.

Great efforts have been put into developing polymer-based fuel cells. Main focus has been on developing fuel cell systems based on the PFSA type membranes where sulfur groups have been inserted into the electrolyte to facilitate proton conduction.

Currently a lot of work have been made on this type of fuel cell. Among others Verbrugge and Verbrugge [1] derived a detailed model based on experimental data. Later Amphlett et al. did a coupled mechanistic and empirical model [2]. Lee et al. presented the influence of CO poisoning on the anode overpotential in [3].

A close relative to the PBI type membrane is the phosphoric acid fuel cell (PAFC) which has been known for the last couple of decades. Data were published regarding the influence of CO concentration in [4].

The use of PBI for fuel cell applications was first published by Wainright et al. [5] followed by a number of papers [6,7].

* Corresponding author. Tel.: +45 96359253; fax: +45 98151411.
E-mail address: ark@iet.aau.dk (A.R. Korsgaard).

0378-7753/$ – see front matter © 2006 Published by Elsevier B.V.
doi:10.1016/j.jpowsour.2006.06.099

Nomenclature

a_x, b_x	Regression constants
F	Faraday constant
I	Cell current
I_0	Exchange current density
R	Universal gas constant
R_{xx}	Resistance
T	Cell temperature
U_0	Open circuit potential

Greek letters

α_c	Transfer coefficient
λ	Cathode stoichiometric ratio

Some of the same authors published data regarding the oxygen reduction reaction in [8] and recently they published data on CO-coverage in [9].

Other research groups also published data regarding development of PBI based MEAs such as the group of Bjerrum and coworkers [10,15,16].

Recently, [11,12] published a model of a PBI membrane but it only included one operating temperature and the stoichiometric ratio was unknown.

If systems and models are to be useable for system design and optimization purposes, detailed documented data are required, but only little has been published. Furthermore, it is necessary to formulate simple yet precise and sufficiently detailed mathematical models based on such experimental experience.

In this paper focus is on the performance of the generic polybenzimidazole (PBI) type MEA from a commercially available source.

Additionally, the data are fitted to a semi empirical model based on pure hydrogen tests including the influence of variations in temperature and cathode stoichiometry, which are the most significant parameters to evaluate system performance.

2. Experimental

The MEAs provided have an active cell area of 45.16 cm^2. The electrode consists of woven graphite fibers and has a thickness of 400 μm. A micro porous layer is coated on the back. The catalyst layer, besides carbon and ionomer, has a platinum loading of 0.7 mg cm^{-2} on the cathode and 1 mg cm^{-2} on the anode. It has a total thickness of 50–100 μm. The membrane itself is 100 μm thick with more than 90 wt.% phosphoric acid in a PBI matrix.

Fig. 1 illustrates the experimental setup, which is based upon a standard test cell. The stainless steel plates contain electrical heating elements in order to control the cell temperature. These are controlled from a computer. The flow plates are made of pure graphite. The flow plates contain three parallel flow serpentine channels on the cathode and two on the anode. The width of each channel is 1.5 mm and the wall thickness is 1 mm.

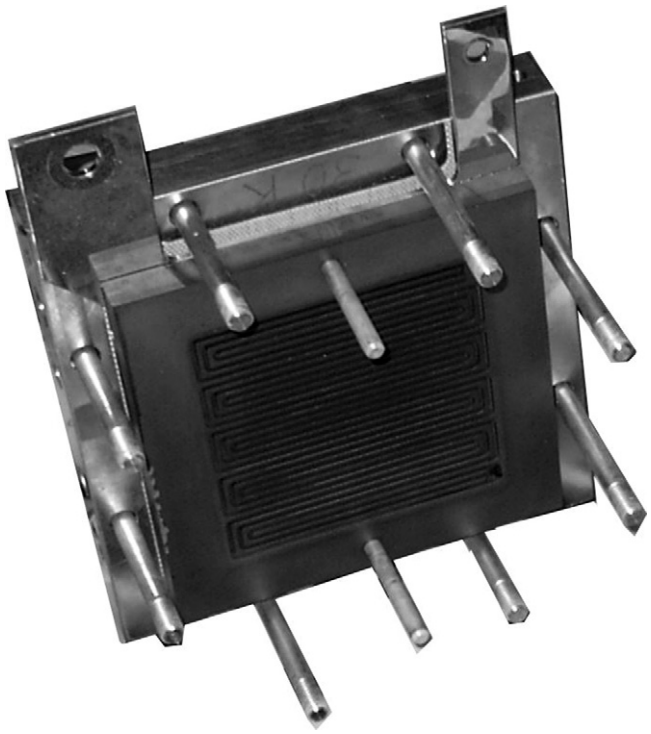

Fig. 1. Picture of test cell.

Fig. 2 shows a schematic representation of the test cell system. Mass flow controllers (of the brand Burkert) were used to control all inlet gases to provide the desired mixture. A water separator was added at the outlet of the test cell. All tests were performed at atmospheric pressure.

A Labview® control and data acquisition system was developed to automatically measure polarization curves. To ensure steady-state conditions, the current was increased by a rate of 30 s A^{-1} until the maximum current of 46 A was reached using a DTI load module (RBL 488). One data sampling was performed each second corresponding to approximately 1500 samples per dataset. The dataset was filtered with a three-point moving average algorithm.

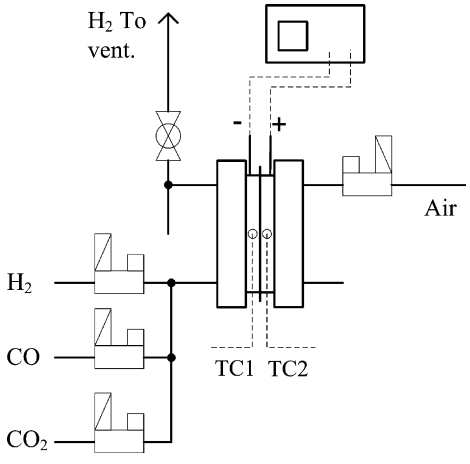

Fig. 2. Schematic of the test setup.

The largest potential measurement error comes from the mass flow controllers (1.8% FS). This will however not affect the measurements since stoichiometric variations in that order will not be readable on the cell voltage. The voltage and current measurements have a relative error less than 0.1%. Hence it is anticipated that differences in the manufacturing process will be the dominating uncertainty in the tests. At small air flows the uncertainty is however much greater, and this can produce measurement errors at low current densities and stoichiometric flows.

To break-in the MEAs they were loaded for 100 h with pure H_2/air with a stoichiometric ratio of 2.5/2.5 at 0.2 A cm^{-2} according to the manufacturer's specifications. During the break-in the performance of the MEA is improved in the order of 20 mV.

The pure hydrogen tests were performed at a stoichiometric ratio of 2.5.

The stoichiometric on the cathode was 2.5 unless otherwise specified.

All synthesis gas tests were performed at high stoichiometric ratios on the anode for two different reasons. First of all the used mass flow controllers for mixing the gases did not have a satisfactory precision at very low flow rates. Moreover, the stoichiometry used in reformer systems will vary greatly with the type of fuel processing technique used, i.e. steam reformer based systems will typically run at higher stoichiometric ratios, while the anode off gas should provide sufficient heat for the burner, than auto thermal or partial oxidation based systems.

The MEA used for the CO tests were replaced in the tests with pure H_2 to prevent any permanent degradation during tests with high CO content at low temperature, influencing the measurements. Additionally, the tests on synthesis gas were performed starting with the higher temperatures for the same reason.

The synthesis gas used was similar to that of a reformed ethanol gas, which has medium carbon content between that of natural gas and diesel.

$$C_2H_5OH + x_3H_2O \rightarrow (2 - x_1)CO_2 + x_2H_2 + x_1CO \quad (1)$$

x_1, x_2 and x_3 express the relative composition of the species in the reactants and products. As can be seen a fixed amount of CO and CO_2 of 25% was maintained while the remaining part is hydrogen. No water was added in these experiments. The CO content was varied according to the following:

- 5% CO, 75% H_2, 20% CO_2;
- 2% CO, 75% H_2, 23% CO_2;
- 1% CO, 75% H_2, 24% CO_2;
- 0.1% CO, 75% H_2, 24.9% CO_2;
- 25% CO_2, 75% H_2;
- 100% H_2.

Tests were also performed at 10% CO but permanent degradation seemed to occur at temperatures below 180 °C.

Tests at 200 °C also permanently degraded the MEA due to the current choice of electrode. Measurement data at this temperature are only provided for the simulated synthesis gas tests.

3. Theory

3.1. Overall model structure

In the present work, a semi empirical model was developed to express the overpotentials in the fuel cell. The expression is extremely simple and has been validated against all the measurement data available.

The cathode activation overpotential is dominant and is based on the Tafel equation. The anode overpotential will be neglected as it is usually very small for pure hydrogen operation as also shown in [1]. Additionally ohmic and concentration losses related to the stoichiometric ratio is expected to exist in the cell. Thus, the overall cell voltage can be written as shown in Eq. (1).

$$U_{cell} = U_0 - \eta_{act} - \eta_{ohmic} - \eta_{diff} \quad (2)$$

This corresponds to the following expression where all the terms are expanded:

$$U_{cell} = \frac{U_0 - RT}{4\alpha_c F} \ln\left(\frac{i + i_0}{i_0}\right) - \frac{R_{ohmic} i - R_{conc} i}{\lambda - 1} \quad (3)$$

The first term, U_0, represents the open circuit voltage and should not be confused with the equilibrium voltage that is sometimes used. The second term is the Tafel equation where i_0 is included in the nominator. This should have a very low impact on the cell voltage but it is incorporated for numerical reasons. The third term is related to ohmic losses, but will also reflect some concentration losses at higher loads.

The last term is a novel approach of including the effect of cathode stoichiometry on performance. As seen this term will approach zero as the stoichiometry goes towards infinity but as it goes towards unity, this term will dominate the result. This is assumed to be in good agreement with the physical behavior of the fuel cell.

3.2. Derivation of regressions

The concentration term in Eq. (3) is physically justified while as λ goes towards 1 this term will completely dominate the cell voltage reduction. The expression, however, is not valid for stoichiometric ratios below 1. As the stoichiometric ratio becomes very high, the influence of this term becomes negligible. The variable R_{conc} is related to the diffusion resistance of the electrode and catalyst layer. It is related to the diffusion coefficient (binary diffusion of O_2 in N_2) and protonic conductivity of the catalyst layer. At higher temperatures this resistance will decrease limiting the influence of this term. A linear regression for the concentration resistance was used as shown in Eq. (4):

$$R_{conc} = a_2 T + b_2 \quad (4)$$

The exchange current density is typically expressed as an exponential function in the form shown in Eq. (5), while Arrhenius type behavior would be expected as the author of [14] suggested.

$$i_0 = a_3 \exp(-b_3 T) \quad (5)$$

The cathode transfer coefficient is assumed to depend on the temperature following a linear relation as [14] and other authors also suggested.

$$a_c = a_0 T + b_0 \quad (6)$$

Note that the actual value of α_c will be lower than the one given by Eq. (6) but this is incorporated open circuit potential.

The protonic conductivity has been given by the manufacturer and has a linear behavior versus temperature ranging from $0.18\,S\,cm^{-1}$ at 100 °C to $0.19\,S\,cm^{-1}$ at 150 °C. The thickness of the membrane is approximately 100 μm. However, not only the membrane contributes to the ohmic losses as the catalyst layer itself is 50–100 μm with a conductivity less than the membrane. At low current densities the reaction takes place relatively close to the membrane but at higher current densities the reaction moves towards the gas diffusion layer as oxygen diffusion limitations begin to dominate. A detailed discussion of this subject is included in the work of Bang et al. [13].

The reaction displacement will result in increasing ohmic losses. It is assumed that the dominating losses will be in the ionomer, consisting of PBI material with the same temperature dependency as the membrane itself. Hence, if the conductivity of the membrane versus temperature can be expressed as a linear regression so can the total ohmic loss:

$$R_{ohmic} = a_1 T + b_1 \quad (7)$$

3.3. Parameter fitting

With the pure hydrogen test data a least square optimization algorithm was used to fit the parameters at each temperature from 120 to 180 °C. Four degrees of freedom were chosen with α, i_0, R_{ohmic} and R_{diff} as the parameters. Then a physical evaluation was done regarding the values of each of the parameters. Afterwards regressions were made stepwise in the following order:

- Linear regression of the diffusion resistance term (R_{diff});
- linear regression of the ohmic resistance (R_{ohmic});
- exponential regression of the exchange current density (i_0);
- linear regression of the charge transfer coefficient (α).

4. Results

4.1. Variation of cathode stoichiometric ratio versus temperature

Fig. 3 shows the tests performed with pure H_2 and air. The stoichiometric ratio was held constant at 2.5 on the anode at all times. It is seen that the performance is significantly improved from 120 to 180 °C. This is due to the better conductivity at higher temperatures. However, at 120 °C it is possible to operate the fuel cell with acceptable performance.

The stoichiometric ratio seems to cause a similar voltage offset at all temperatures even though the overpotential is slightly higher at lower temperatures. This could be due to the fact that

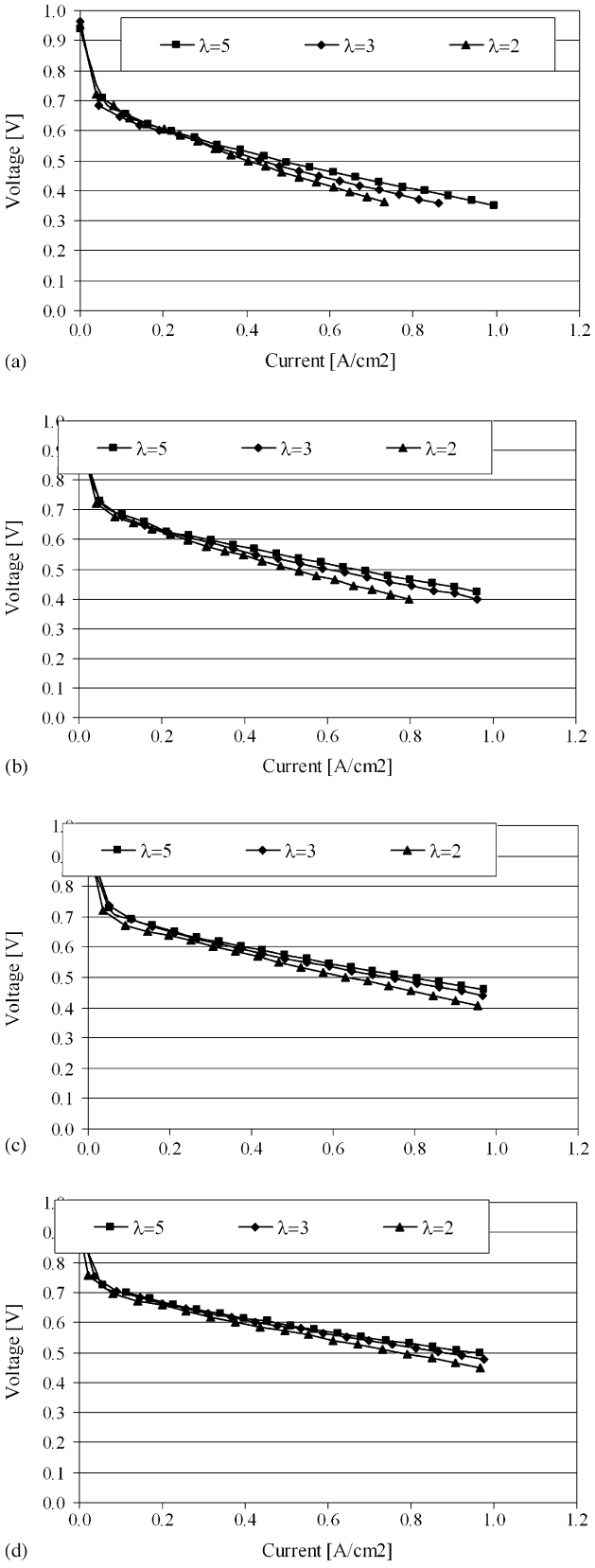

Fig. 3. Test results for pure H_2 and air at temperatures (a) 120 °C, (b) 140 °C, (c) 160 °C and (d) 180 °C.

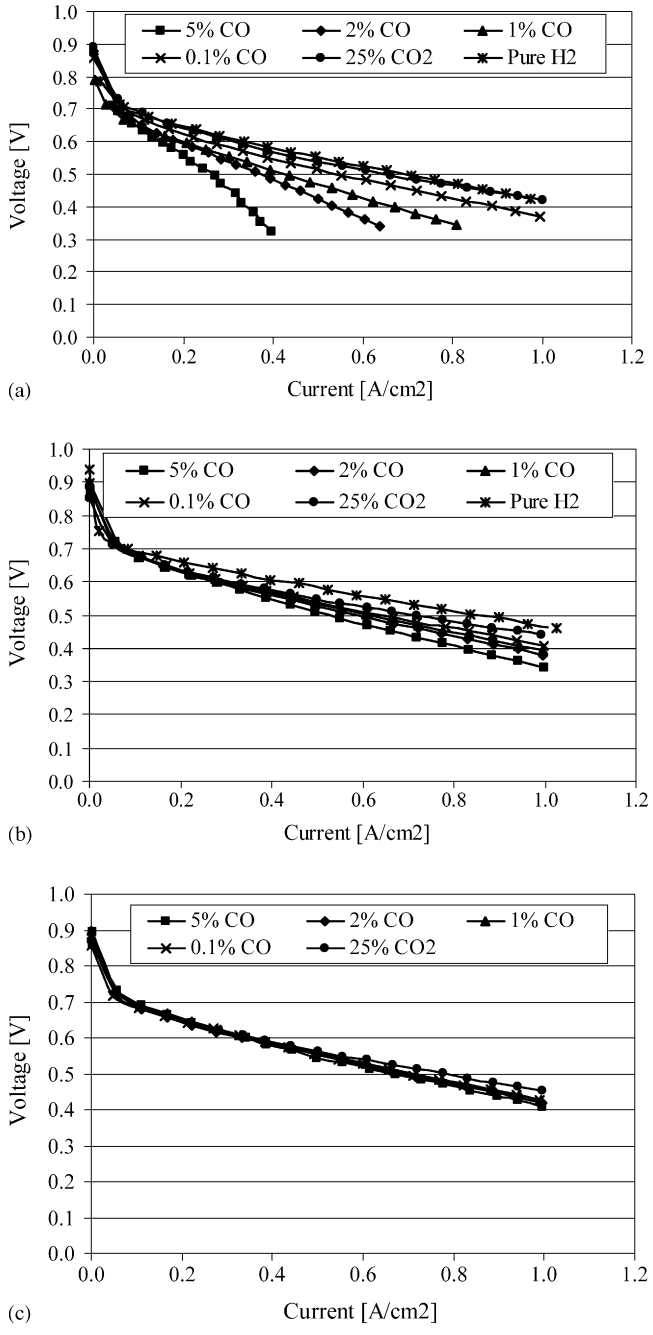

Fig. 4. Test results for synthesis mixture compared to pure H_2 curves for temperatures (a) 160 °C, (b) 180 °C and (c) 200 °C.

the oxygen diffusion coefficient in air increases with temperature and thereby decreasing the cathode overpotential.

4.2. Synthesis gas influence anode overpotentials

Fig. 4 shows the tests performed on synthesis gas at 160, 180 and 200 °C.

At 160 °C and 5% CO, the cell performance is significantly affected but at 2% CO the operation seemed stable though a performance decrease is clear. By lowering the CO concentration to 1% and below, cell performance is considerably improved.

The carbon monoxide impact is also reduced at 180 °C and the fuel cell is stable at all operating conditions, even though performance is still significantly reduced. At 200 °C only limited performance degradation was observed when varying the CO content. The presence of CO_2 had only negligible effect on the performance.

4.3. Model fit of pure hydrogen tests versus temperature and cathode stoichiometry

Fig. 5 shows the modeling results for the pure hydrogen tests. Results for stoichiometric ratios 2, 3 and 5 are shown. In each of the plots, four temperature curves are shown with both experimental and model results. The lowest cell potential corresponds

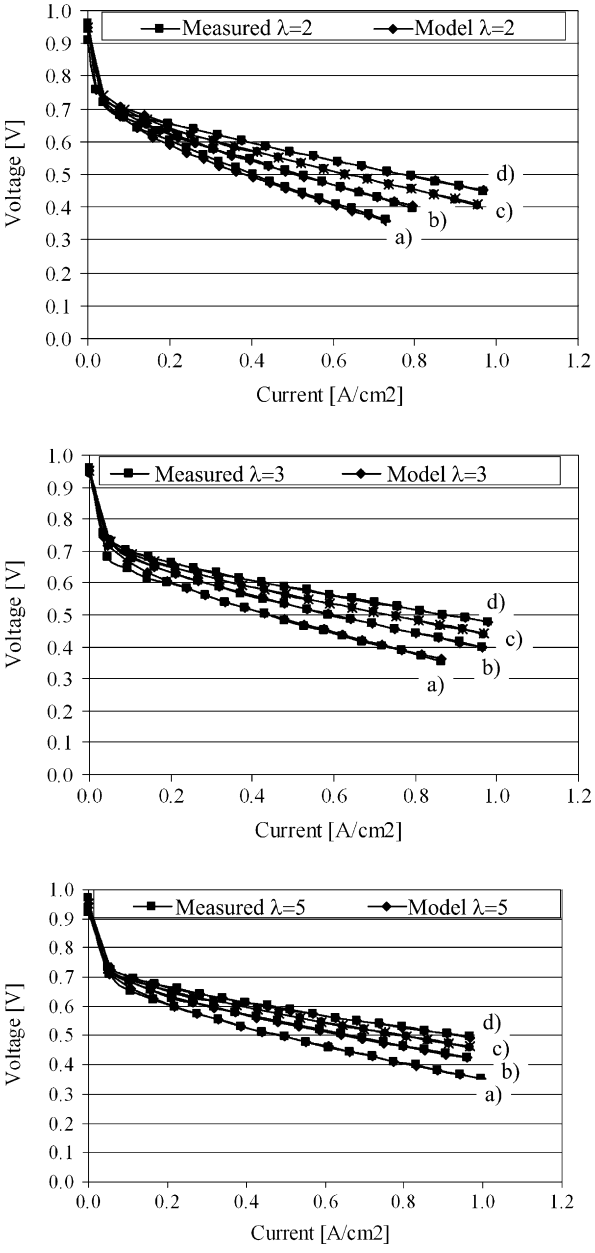

Fig. 5. Modeling results for pure hydrogen vs. specific current, stoichiometric ratio and temperatures from (a) 120 °C, (b) 140 °C, (c) 160 °C and (d) 180 °C.

Table 1
Numerical values used in model

Membrane	
Membrane thickness, t_{memb}	0.1×10^{-3} m
Values used for regressions	
Charge transfer constant, a_0	2.712×10^{-3} K^{-1}
Charge transfer constant, b_0	−0.9049
Ohmic loss constant, a_1	−0.0006488 Ω K^{-1}
Ohmic loss constant, b_1	0.4410 Ω
Diffusion limitation constant, a_2	−0.001106 Ω K^{-1}
Diffusion limitation constant, b_2	0.5569 Ω
Limiting current constant, a_3	33.3×10^3 A
Limiting current constant, b_3	−0.04506
Open circuit voltage, U_0	0.95 V
Other values	
Universal gas constant, R	8.3143 J mol^{-1} K^{-1}
Faradays constant, F	96485 C mol^{-1}

to the lowest cell temperature and upwards. As it is seen, a very good agreement between model and experiments was achieved. The overall average error was only 5 mV. The errors in the low ranges of the current density can be explained by the turn down ratio of the mass flow controller. It is within its nominal operating range at currents larger than 0.1 A cm^{-2}. Table 1 shows the values of the parameters derived during the fitting procedure.

5. Discussion

5.1. Experimental results

It is seen that the CO surface coverage is highly temperature dependent. This was however also expected as the kinetics favor CO-desorption at higher temperatures. The reason for the minor CO_2 performance degradation is not entirely understood. Possibly, the water–gas-shift reaction plays a role. The presence of water at both the anode and cathode compartments was observed during the experiments. The experiments performed show good agreement with the results of [15,16]. As explained the experiments with synthesis gas were made at high anode stoichiometric ratios. Hence the results cannot directly related to.

Future tests with an inert gas such as nitrogen will reveal the ad-/de-sorption kinetics dominating the performance.

It is also shown that increasing operating temperature and stoichiometric ratio significantly enhances the performance. However, these parameters might also limit lifetime of the MEA. Upcoming studies will reveal the relationship between these operating conditions and degradation and MEA failure.

5.2. Modeling results

It was found that the total ohmic losses were approximately three times what the resistance of the membrane itself would predict, which is believed to be realistic. Additionally, the transfer coefficient was found to be in the range from 0.14 at 120 °C to 0.32 at 180 °C. This is in the lower region compared to what is typically published for low temperature PEM MEAs. It should be stressed however that these values cannot be directly related to the values given in other literature, as the open circuit is used instead of the equilibrium voltage.

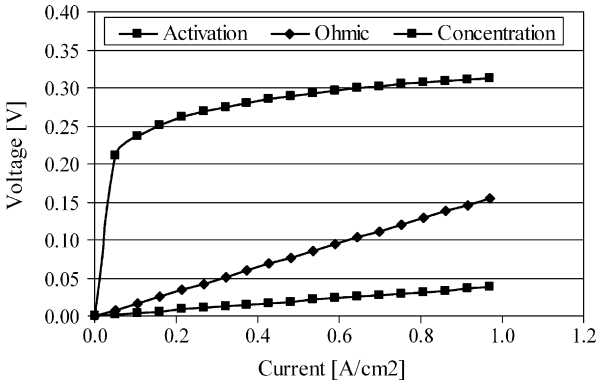

Fig. 6. Distribution of overpotentials vs. current at 160 °C and a cathode stoichiometry of 3.

The slope of the charge transfer coefficient however, is found to be 0.0028 which is in perfect agreement with the work carried out by Parthasarthy et al. [14]. They measured the slope of the charge transfer coefficient to be 0.0023 for Nafion, and referred to other publications for phosphoric acid fuel cells where the rate is between 0 for 98% H_3PO_4 and 0.0034 for 85% H_3PO_4.

The ohmic resistance is also believed to be of a realistic magnitude compared to the published data for the MEA itself.

A model of the anode kinetics as well as a detailed model of the catalyst layer is being developed.

Fig. 6 shows the loss distribution in terms of activation, ohmic and the concentration losses related to the cathode stoichiometry. Comparing to the work of [12] the ohmic losses contribute much more to the total losses. This could be due to the fact that the catalyst layer protonic loss was not included in their work. The concentration loss also has a significant loss associated while the activation losses are lower. This however, is caused by the use of the open circuit voltage in Eq. (3) instead of the equilibrium voltage as previously discussed.

6. Conclusions

Tests were performed on commercial intermediate temperature MEAs based on the polybenzimidazole membrane. The influence on cell performance of operating parameters such as cathode stoichiometric ratio and operating temperature were investigated.

It was found that it is possible to operate the fuel cell from 160 °C with a CO content of up to 2%. Even higher CO concentrations are possible but operation at these temperatures requires an increase of temperature.

A very simple model of the cell voltage was developed based on pure hydrogen tests, which will be very useful in any system model. It agrees very well with an average error on each point less than 4 mV in the range from 120 to 180 °C and stoichiometric ratios from 2 to 5. A novel method for modeling the influence of cathode stoichiometry was also included with very good results.

In general the model is very suitable for applications such as system modeling, control design or for use in real-time applications.

Acknowledgements

The authors would like to thank a number of companies supporting the work including Dantherm, Danfoss and APC Denmark.

References

[1] D.M. Verbrugge, M.W. Verbrugge, J. Electrochem. Soc. 139 (1992) 2477–2490.
[2] J.C. Amphlett, R.M. Baumert, R.F. Mann, B.A. Peppley, P.R. Roberge, J. Electrochem. Soc. 142 (1995) 1–8.
[3] S.J. Lee, S. Mukerjee, E.A. Ticianelli, J. McBreen, Electrochim. Acta 44 (1999) 3283–3293.
[4] Rak-Hyun Song, Dong Ryul Shin, Int. J. Hydrogen Energy 26 (2001) 1259–1262.
[5] J.S. Wainright, J.-T. Wang, D. Weng, R.F. Savinell, M. Litt, J. Electrochem. Soc. 142 (1995) 121–123.
[6] R.F. Savinell, J.S. Wainright, M. Litt, Electrochem. Soc. (1995) 214–215.
[7] J.T. Wang, R.F. Savinell, J.S. Wainright, M. Litt, H. Yu, Electrochim. Acta 41 (1996) 193–197.
[8] Zhenyu Liu, Jesse S. Wainright, Robert F. Savinell, Chem. Eng. Sci. 59 (2004) 4833–4838.
[9] J.D. Holladay, J.S. Wainright, E.O. Jones, S.R. Gano, J. Power Sources 130 (2004) 111–118.
[10] Qingfeng Li, et al., Solid State Ionics 168 (2004) 177–185.
[11] D. Cheddie, N. Munroe, J. Power Sources 156 (2006) 414–423.
[12] D. Cheddie, N. Munroe, Energy Convers. Manage. 47 (2006) 1490–1504.
[13] M. Bang, M. Odgaard, T.J. Condra1, S.K. Kær, ASME Fuel Cell (2004).
[14] A. Parthasarthy, S. Srinivasan, A.J. Appleby, J. Electrochem. Soc. 139 (1992) 2530–2537.
[15] Q. Li, R. He, J.O. Jensen, N.J. Bjerrum, Fuel Cells 4 (3) (2004) 147–159.
[16] Li Qingfeng, H.A. Hjuler, N.J. Bjerrum, J. Appl. Electrochem. 31 (7) (2001) 773–779.